HRX-SAFT Equation of State for Fluid Mixtures: New Analytical Formulation†

Sergei B. Kiselev and James F. Ely*

Chemical Engineering Department, Colorado School of Mines, Golden, Colorado 80401-1887

Received: May 15, 2007; In Final Form: August 14, 2007

In this work, we incorporate the new analytical sine model (ANS) crossover function (Kiselev and Ely, *Chem. Eng. Sci.* **2006**, *61*, 5107.) into the previously developed crossover statistical associating fluid theory (HRX-SAFT) equation of state (EOS) (Kiselev et al. *Ind. Eng. Chem. Res*. **2006**, *45*, 3981.). Similar to the original HRX-SAFT EOS, the new crossover HRX/ANS EOS incorporates non-analytic scaling laws in the critical region and is transformed into the analytical, classical HR-SAFT EOS far away from the critical point. The new HRX/ANS EOS does not, however, require a numerical solution for the crossover function, making it much simpler and more convenient for practical calculations. In this work, the HRX/ANS-SAFT mixture model is developed and tested against extensive experimental data for VLE, PVTx, and excess properties in carbon dioxide + methanol and water + methanol mixtures.

1. Introduction

The statistical associating fluid theory (SAFT) equations of state (EOS) proposed in the late 1980s by Gubbins and co-workers[1−3] and its engineering version proposed by Huang and Radosz (HR-SAFT)[4−9] are probably the first molecular-based equations for associating fluids with strong attractive interactions between molecules. On the basis of the thermodynamic perturbation theory of Werthiem,[10−13] the SAFT equations[1−9] and their different modifications[14,15] appear to be an effective tool for describing thermodynamic properties and phase equilibria of associating and complex fluids. However, similar to all analytical EOS, the SAFT equations are essentially mean field equations that fail to reproduce the non-analytical, singular behavior of fluids in the critical region caused by long-scale fluctuations in density. In order to incorporate the critical fluctuations, the original analytical equations should be renormalized. During the last two decades, many efforts have been made to develop a "global" or generalized EOS that at low densities reproduces the ideal gas equation and is transformed into the non-analytic scaled EOS as the critical point is approached.[16−42] The most theoretically advanced models are probably the hierarchical reference theory (HRT) developed by Parola and co-workers[29−31,34,36,43] and the "globalized" renormalization-group (RG) procedure proposed by White and co-workers.[38−42] An advantage of the HRT and "globalized" RG models is that they require only a few microscopic intermolecular potential parameters as input. However, they are rather complicated and require additional spline functions for the practical representation of the thermodynamic surface of real fluids.

A general renormalization-group theory based procedure for incorporating long-range density fluctuations into any classical-analytical equation was proposed by Kiselev.[44] During the last 5 years, this procedure has been applied successfully to different types of equations of state, including cubic,[45−48] SAFT,[43,49−55] and empirical multiparameter equations.[56]

In our previous work, we used this procedure to develop a crossover SAFT EOS (HRX-SAFT) for binary mixtures of associating fluids.[53] In that work, we have shown that the HRX-SAFT EOS not only better reproduces the VLE properties of binary mixtures in the critical region than the classical HR-SAFT EOS but also yields a very good description of the excess properties as well. However, the HRX-SAFT EOS obtained in ref 53 was based on the crossover sine model[57] and requires a numerical solution of a transcendental equation for the crossover function. This makes the calculation of the crossover function and its first and second derivatives rather complicated and restricts its widespread practical application for engineering calculations.

To overcome this shortcoming of the original HRX-SAFT EOS,[53] we have developed a modified HRX/ASN-SAFT EOS based on an analytical formulation of the sine model (ASN).[58] In this work, we have used the HRX/ASN-SAFT equation of state for thermodynamic calculations for pure carbon dioxide, water, and methanol and, using classical mixing rules in term of composition, we have applied the HRX/ASN-SAFT EOS to binary carbon dioxide/methanol and water/methanol mixtures.

We proceed as follows. In Section 2, we describe an original SAFT EOS for mixtures and describe a general procedure for transforming it into the crossover form. In Section 3, we develop the HRX/ASN-SAFT EOS for pure components and binary mixtures and provide comparisons with experimental data. Our results are summarized and discussed in Section 4.

2. Thermodynamic Model

2.1. Classical SAFT Equation of State for Mixtures. For the classical SAFT EOS we used the same formulation as was employed in our previous work.[53] A brief description of HR-SAFT for mixtures is given here, and readers are referred to the original paper for details.[6] The residual Helmholtz energy is a sum of terms that represent the repulsive and attractive interactions in the system

† Part of the "Keith E. Gubbins Festschrift".

* To whom correspondence should be addressed. E-mail jely@mines.edu.

10.1021/jp073706p CCC: $37.00
Published on Web 10/25/2007

$$a^{\mathrm{res}} = \frac{A^{\mathrm{res}}}{n_{\mathrm{m}}RT} = a^{\mathrm{hs}} + a^{\mathrm{disp}} + a^{\mathrm{chain}} + a^{\mathrm{assoc}} \quad (1)$$

where A is the Helmholtz energy, a is the dimensionless Helmholtz energy, n_{m} is the number of moles, R is the gas constant, T is the absolute temperature, and the superscripts stand for residual, hard-sphere, dispersion, chain, and association, respectively.

The mixture hard-sphere term was given by Mansoori et al.[59]

$$a^{\mathrm{hs}} = \frac{6}{\pi\rho N_{\mathrm{A}}}\left[\frac{(\zeta_2)^3 + 3\zeta_1\zeta_2\zeta_3 - 3\zeta_1\zeta_2(\zeta_3)^2}{\zeta_3(1-\zeta_3)^2} - \left(\zeta_0 - \frac{(\zeta_2)^3}{(\zeta_3)^2}\right)\ln(1-\zeta_3)\right] \quad (2)$$

where

$$\zeta_k = \frac{\pi}{6} N_{\mathrm{A}}\rho \sum_i x_i\, m_i\, d_i^{\,k} \quad (3)$$

In eqs 2 and 3 N_{A} is Avogadro's number, ρ is the molar density, m_i is the number of segments in component i, d_i is the temperature-dependent segment diameter of component i, and x_i is the mol fraction of component i.

For the dispersion term, we use the equation proposed by Chen and Kreglewski[60]

$$a^{\mathrm{disp}} = \left(\sum_i x_i\, m_i\right) \sum_{m=1}^{4}\sum_{n=1}^{9} D_{mn}\left(\frac{u}{kT}\right)^m\left(\frac{\zeta_3}{\tau}\right)^n \quad (4)$$

where $\tau = 0.74048$ and D_{mn} are universal constants[5] and

$$\frac{u}{kT} = \frac{\sum_i\sum_j x_i\, x_j\, m_i\, m_j\left[\frac{u_{ij}}{kT}\right](v^{\mathrm{o}})_{ij}}{\sum_i\sum_j x_i\, x_j\, m_i\, m_j (v^{\mathrm{o}})_{ij}} \quad (5)$$

$$(v^{\mathrm{o}})_{ij} = \left[\frac{1}{2}\left[(v^{\mathrm{o}})_i^{1/3} + (v^{\mathrm{o}})_j^{1/3}\right]\right]^3 \quad (6)$$

$$u_{ij} = (1-k_{ij})(u_i u_j)^{1/2} \quad (7)$$

Here, k_{ij} is a binary interaction parameter that is fitted to experimental data and $(v^{\mathrm{o}})_i$ is the temperature-dependent segment volume of pure component i in a closed-packed arrangement.

The chain contribution is is given by

$$a^{\mathrm{chain}} = \sum_i x_i(1-m_i)\ln g^{\mathrm{hs}}(d_i) \quad (8)$$

where $g^{\mathrm{hs}}(d_i)$ is the radial distribution function for hard-sphere fluid mixtures evaluated at contact

$$g^{\mathrm{hs}}(d_i) = \frac{1}{1-\zeta_3} + \frac{3d_i}{2}\frac{\zeta_2}{(1-\zeta_3)^2} + 2\left[\frac{d_i}{2}\right]^2\frac{(\zeta_2)^2}{(1-\zeta_3)^3} \quad (9)$$

The association term is given by

$$a^{\mathrm{assoc}} = \sum_{i=1}^{n} x_i \sum_{j=1}^{s} S_i^{\,j}\left(\ln(X_i^{\,j}) - (1/2)X_i^{\,j} + (1/2)\right) \quad (10)$$

where the fraction of associating molecules i not bonded at site j is given by the mass-action equation

$$X_i^{\,j} = \frac{1}{1 + \rho N_{\mathrm{A}}\sum_{k=1}^{n} x_k \sum_{l=1,l\neq j}^{s} S_k^{\,l} X_k^{\,l}\Delta_{ki}^{lj}}, \qquad i = 1,...,n;\ j = 1,...,s \quad (11)$$

In eqs 10 and 11, $S_i^{\,j}$ is the number of association sites of type j in each molecule of component i, n is the number of components in the mixture, s is the number of association-site types, and Δ_{ki}^{lj} is the association strength between site type l in component k and site type j in component i approximated by[1]

$$\Delta_{ki}^{lj} = \kappa_{ki}^{lj} g^{\mathrm{hs}}(\sigma_{ki})\left(\exp\left(\frac{\epsilon_{ki}^{lj}}{kT}\right) - 1\right) \quad (12)$$

κ_{ki}^{lj} is a measure of the volume available for bonding between site of type l in component k with site of type j in component i, ϵ_{ki}^{lj} is the well depth of the site−site interaction potential between site of type l in component k with site of type j in component i, $g^{\mathrm{hs}}(\sigma_{ki})$ is the hard-sphere pair correlation function evaluated at contact, and σ_{ki} is the segment diameter for the $k-i$ pair.

We use the generalized procedure proposed by Tan et al.[61] to calculate the fractions of nonbonded associating molecules and their derivatives. In that procedure, the high-order derivatives of $X_i^{\,j}$ are very simple to obtain and can be written in a matrix form

$$[\Lambda_{pq}]\left[\frac{\partial^m}{\partial y_1\partial y_2\cdots\partial y_m}[X_i^{\,j}]\right] = [\Psi_p^{y_1y_2\cdots y_m}] \quad (13)$$

where the y's denote thermodynamic variables (e.g., density, temperature, etc.), the matrix $[\Lambda_{pq}]$ has an order of $(s\times n)\times(s\times n)$ with

$$p = n(j-1) + i \qquad i = 1,...,n;\ j = 1,...,s$$
$$q = n(l-1) + k \qquad k = 1,...,n;\ l = 1,...,s \quad (14)$$

and the other two matrices are of order $(s\times n)\times 1$. As described in Tan et al.,[61] the elements of matrix $[\Lambda_{pq}]$ do *not* depend on variables y_n, but those of matrix $[\Psi_p^{y_n}]$ do. The expression for $[\Lambda_{pq}]$, as well as those for the matrices $[\Psi]$ for first-order derivatives and commonly used second-order derivatives of $X_i^{\,j}$, are given in ref 48. Matrices $[\Psi]$ for the third-order derivatives needed in this work are given in the Appendix.

2.2. Crossover HR-SAFT Equation of State. The general procedure for transforming an analytical EOS into the crossover form has been described in detail elsewhere.[44,45] Following that approach, we first formally split the dimensionless classical Helmholtz free energy $a(T,v)$ for the HR-SAFT EOS in two contributions

$$a(T,v) = \Delta\, a(\Delta T,\Delta v) + a_{\mathrm{bg}}(T,v) \quad (15)$$

where the critical, $\Delta a(\Delta T,\Delta v)$, and background, $a_{\mathrm{bg}}(T,v)$, parts are given by

$$\Delta a(\Delta T,\Delta v) = a^{\mathrm{res}}(\Delta T,\Delta v) - a_0^{\mathrm{res}}(\Delta T) + \bar{P}_0(\Delta T)\Delta v - \ln(\Delta v + 1) \quad (16)$$

$$a_{\mathrm{bg}}(T,v) = a_0^{\mathrm{res}}(T) - \bar{P}_0(T)\Delta v + a^{\mathrm{id}}(T) \quad (17)$$

TABLE 1: System-Dependent Parameters in the HRX/ASN-SAFT EOS for Pure Components

parameter	CO_2	H_2O	CH_3OH
v^{oo} (mL·mol^{-1})	4.58025954	1.02398431×10^1	1.05485552×10^1
m	3.94062349	1.33799081	2.00840438
u^0/k_B (K)	1.23942057×10^2	2.91816303×10^2	1.83917636×10^2
ϵ/k_B (K)	1.07689612×10^3	2.83035448×10^3	2.80763795×10^3
κ	$1.20079313 \times 10^{-3}$	$7.46778013 \times 10^{-2}$	$6.52979794 \times 10^{-2}$
Gi	$8.42356847 \times 10^{-2}$	$2.30763914 \times 10^{-1}$	$1.05693778 \times 10^{-1}$
v_1	$3.19204522 \times 10^{-3}$	$7.61234381 \times 10^{-4}$	$7.20941922 \times 10^{-3}$
m_0	1.43628985	1.44056771	2.55718182
M_w	44.010	18.0152	32.0420
[a] T_c (K)	304.120	647.096	512.750
[b] r_c (mol·l^{-1})	10.7625	17.8738	8.27000
[b] P_c (bar)	73.7900	220.631	81.2008
N sites	2	3	2

[a] Experimental values adopted from Table 1 in ref 45. [b] Calculated with the HRX/SAN- SAFT EOS.

TABLE 2: System-Dependent Parameters in the HRX/ASN-SAFT EOS for Mixtures

parameter	$CO_2(1) + CH_3OH(2)$	$H_2O(1) + CH_3OH(2)$
k_{12}	1.5×10^{-1}	6.8021930×10^{-2}
ϵ_{12}^{13}/k_B (K)	[a] 2.80763795×10^3	3.07029712×10^3
κ_{12}^{13}	3.0×10^{-3}	1.8912270×10^{-2}

[a] The coefficient $\epsilon_{12}^{13} = \epsilon$ for pure methanol.

$\Delta T = T/T_{0c} - 1$ and $\Delta v = v/v_{0c} - 1$ are dimensionless distances from the classical critical temperature T_{0c} and molar volume v_{0c}, respectively, $\bar{P}_0(T) = P_0(T,v_{0c})v_{0c}/RT$ is the dimensionless pressure, $a_0^{res}(T) = a^{res}(T,v_{0c})$ is the dimensionless residual part of the Helmholtz energy along the critical isochore $v = v_{0c}$, and $a^{id}(T)$ is the dimensionless temperature-dependent ideal-gas Helmholtz free energy.

In the second step, we replace the classical values of ΔT and Δv in the critical part $\Delta a(\Delta T,\Delta v)$ with the renormalized values[52,57]

$$\bar{\tau} = \tau Y^{-\alpha/2} + (1+\tau)\Delta T_c Y^{2(2-\alpha)/3} \quad (18)$$

$$\bar{\varphi} = \varphi Y^{(\gamma-2\beta)/4} + (1+\varphi)\Delta v_c Y^{(2-\alpha)/2} \quad (19)$$

where $\alpha = 0.11$, $\beta = 0.325$, and $\gamma = 2 - 2\beta - \alpha = 1.24$ are universal nonclassical critical exponents,[62,63] $\tau = T/T_c - 1$ is a dimensionless deviation of the temperature from the true critical temperature T_c, $\varphi = v/v_c - 1$ is a dimensionless deviation of the molar volume from the true critical molar volume v_c, $\Delta T_c = (T_c - T_{0c})/T_{0c} \ll 1$ and $\Delta v_c = (v_c - v_{0c})/v_{0c} \ll 1$ are dimensionless shifts of the critical temperature and volume, respectively, and $Y(q) = \Upsilon(q)^{1/\Delta_1}$ denotes a crossover function. In this work,we use a simple phenomenological expression obtained by Kiselev et al. [43,44,52,57,64] for the crossover function Y

$$Y(q) = \left(\frac{q}{1+q}\right)^2 \quad (20)$$

Unlike our work for the HRX-SAFT EOS,[53] the renormalized distance to the critical point q is found from a solution of the analytical sine (ASN) model[58]

$$q^2 = \frac{4\left(\frac{b}{m_0}\left|\hat{\varphi}\right|\right)^{1/\beta} + 2\tau + \sqrt{\left[4\left(\frac{b}{m_0}\left|\hat{\varphi}\right|\right)^{1/\beta} + 2\tau\right]^2 + 12\tau^2}}{6Gi} \quad (21)$$

where $\hat{\varphi} = \varphi[1 + v_1 \exp(-10\eta)] + d_1\tau$, the coefficients m_0, v_1, d_1, and the Ginzburg number Gi are the system-dependent parameters, and the parameter $b^2 = b_{LM}^2 \cong 1.359$ a the universal linear model (LM) parameter.[57] The crossover sine model as given by eq 21 is physically equivalent to that developed earlier[52,57,64] but with a different empirical term $\propto v_1 \exp(-10\varphi)$,[45] which provides the physically obvious condition $Y = 1$ at the triple point of liquids. Finally, the HRX/ANS-SAFT expression for the Helmholtz free energy can be written in the form

$$a(T,v) = \Delta\, a(\bar{\tau},\bar{\varphi}) - \Delta v\bar{P}_0(T) + a_0^{res}(T) + a^{id}(T) \quad (22)$$

On the basis of the principle of the critical point universality,[65-67] a mixture crossover EOS that reproduces known scaling laws must have mixing rules formulated in terms of the "field" variables (the chemical potential of a mixture $\mu = \mu_2 - \mu_1 = (\partial A/\partial x)_{T,v}$) rather than the "density" variables (the composition x). This development, however, makes mixture calculations complicated and time-consuming. Thus, in this work, similar to the crossover HRX-SAFT EOS,[53] we adopted the mixing rules in terms of composition. In this case the parameters parameters T_c, P_c, and v_c in the HRX-SAFT EOS for the mixtures are pseudo-critical parameters, and the classical critical molar density and temperature, that is, $\rho_{0c}(x)$ and $T_{0c}(x)$, are obtained by solving the criticality conditions

$$\left(\frac{\partial P}{\partial \rho}\right)_{x,T^{0c}} = \left(\frac{\partial^2 P}{\partial \rho^2}\right)_{x,T_{0c}} = 0 \quad (23)$$

where the crossover equation of state can be obtained by differentiation of eq 23 with respect to volume

$$P(v,T,x) = -RT\left(\frac{\partial a}{\partial v}\right)_{x,T} = \frac{RT}{v_{0c}}\left\{-\frac{v_{0c}}{v_c}\left(\frac{\partial \Delta\, a}{\partial \varphi}\right)_{x,T} + \bar{P}_0(T)\right\} \quad (24)$$

Once ρ_{0c} and T_{0c} are known, the critical pressure P_{0c} can also be obtained.

3. Comparison with Experimental Data

3.1. Pure Components. In order to apply the HRX/ASN-SAFT EOS to mixture calculations, one needs first to know the pure component parameters. The HRX/ASN-SAFT EOS for pure fluids contains five classical parameters, namely, the segment number m, the segment volume v^{oo} (or σ), the segment energy u^o, the well depth of site−site potential ϵ, and the volume bonding parameter κ, and four crossover parameters, the

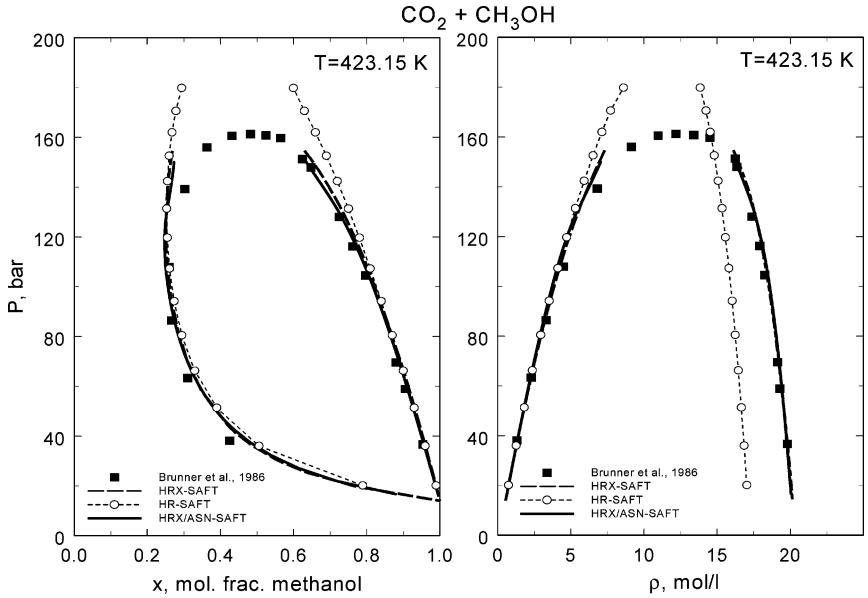

Figure 1. Pressure−composition (left) and pressure−density (right) VLE isotherms for carbon dioxide + methanol mixture. The curves correspond to the HRX/ASN-SAFT (solid curves) and HRX-SAFT (dashed curves) model, open circles with dashed curves represent the values calculated with the classical HR-SAFT EOS, and the filled symbols indicate the experimental data.[69]

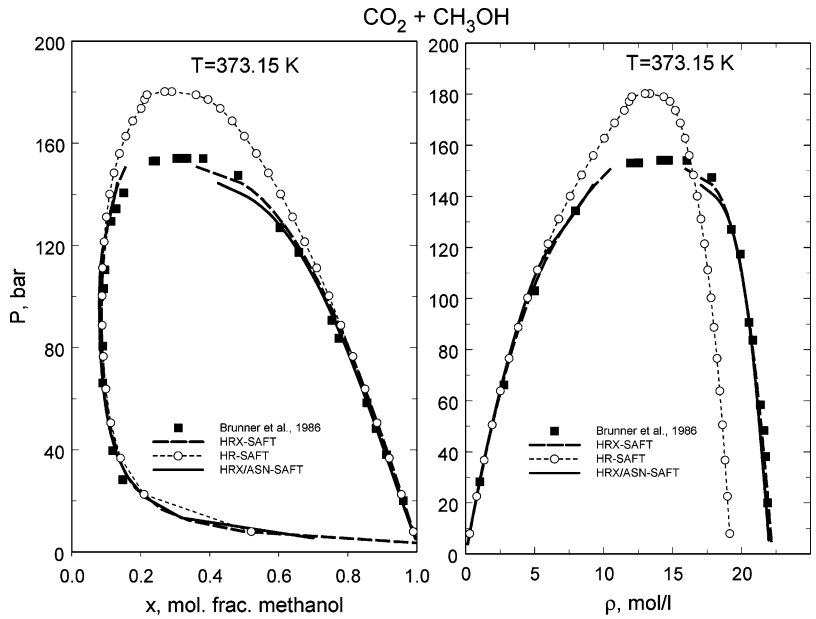

Figure 2. Pressure−composition (left) and pressure−density (right) VLE isotherms for carbon dioxide + methanol mixture. The curves correspond to the HRX/ASN-SAFT (solid curves) and HRX-SAFT (dashed curves) model, open circles with dashed curves represent the values calculated with the classical HR-SAFT EOS, and the filled symbols indicate the experimental data.[69]

coefficients m_0, v_1, d_1, and the Ginzburg number Gi. In order to reduce the number of the adjustable parameters, we have set $d_1 = 0$.[53] Thus, the HRX/ASN-SAFT EOS for pure fluids contains eight parameters, which for all substances have been found from a fit of the model to the VLE and one-phase PVT data. Because carbon dioxide has a strong quadrupole moment, it can form complexes with water and methanol. Therefore, following Button and Gubbins,[68] we also consider carbon dioxide to be an associating fluid with the association sites being on the oxygens. Methanol and water were assumed to have two hydrogen-bonding sites associated with each −OH structure. All system-dependent parameters for pure carbon dioxide, water, and methanol are listed in Table 1.

Because the results for methanol are very similar to those obtained in our previous work,[53] they are not repeated here. For all three substances, the HRX/ASN-SAFT EOS reproduces the vapor pressure data from the triple point to the critical temperature with an average absolute deviation (AAD) of about 1%, the saturated liquid and vapor densities with an AAD of about 1−3%, and the single-phase pressures in the one-phase region with an AAD of about 2−3%.

3.2. Binary Mixtures. As mentioned above, we have adopted mixing rules based on composition rather than the field variables and we have assumed that carbon dioxide exhibits non-hydrogen-bonding association at two sites. Methanol and water were assumed to have hydrogen-bonding sites on the hydrogen and oxygen. Following our previous work,[53] for the

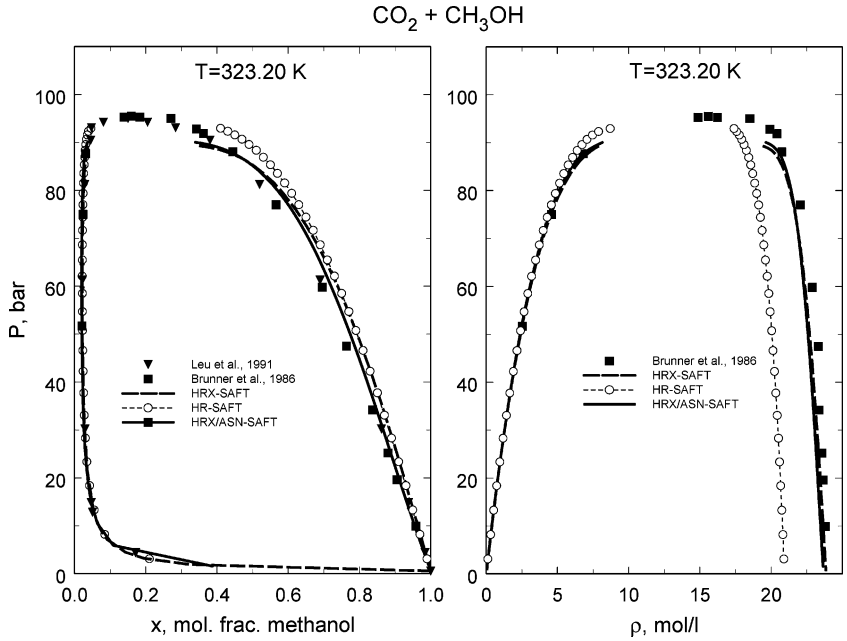

Figure 3. Pressure−composition (left) and pressure−density (right) VLE isotherms for carbon dioxide + methanol mixture. The curves correspond to the HRX/ASN-SAFT (solid curves) and HRX-SAFT (dashed curves) model, open circles with dashed curves represent the values calculated with the classical HR-SAFT EOS, and the filled symbols indicate the experimental data.[69,74]

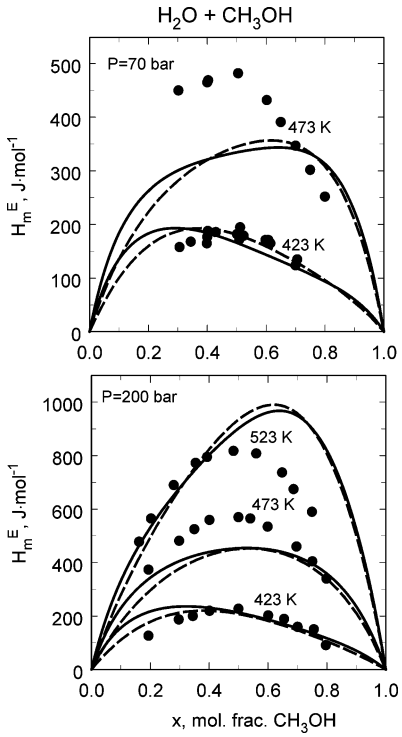

Figure 4. Excess molar enthalpy H_m^E as a function of composition for water + methanol mixture at $P = 70$ bar (top) and 200 bar (bottom) and different temperatures. The curves correspond to the HRX/ASN-SAFT (solid curves) and HRX-SAFT (dashed curves) models,[53] and the symbols indicate the data of Wormald et al.[73]

cross interaction in the carbon dioxide (1) + methanol (2) mixtures we set

$$\kappa_{12}^{21} = 0, \epsilon_{12}^{21} = 0 \qquad (25)$$

In water and methanol the interaction is hydrogen bonding; therefore, for the cross-interaction parameters in water (1) + methanol (2) mixtures we set

$$\kappa_{12}^{31} = \kappa_{12}^{13}, \qquad \epsilon_{12}^{31} = \epsilon_{12}^{13} \qquad (26)$$

In all cases, the Ginzburg number Gi and coefficients m_0, v_1, and d_1 (marked below as k_1) we used simple linear relationships

$$\frac{1}{Gi(x)} = \frac{1-x}{Gi^{(0)}} + \frac{x}{Gi^{(1)}}, \qquad k_1(x) = k_1^{(0)}(1-x) + k_1^{(1)}x \qquad (27)$$

(where superscripts "0" and "1" denote the first and second components of the mixture, respectively), and the coefficients κ_{12}^{13} and ϵ_{12}^{13} were treated as adjustable parameters of the model. Values of the system-dependent parameters in the HRX/ASN-SAFT EOS for binary mixtures are listed in Table 2.

The first system that we consider here is the carbon dioxide + methanol mixture. In this mixture, we adopted the same value for the coefficient κ_{12}^{13} as obtained earlier using the HRX−SAFT EOS,[53] the coefficient ϵ_{12}^{13} was set equal to the coefficient ϵ_{AB} for pure methanol, and the coefficient k_{12} was found from optimization of the HRX/ASN-SAFT EOS to the $P - x$ VLE data at $T = 423.15$ K reported by Brunner et al.[69] The comparisons of the experimental data with the values calculated with the HRX/ASN-SAFT model are shown in Figure 1. The empty circles with eye-guide lines in Figure 1 represent the values calculated with the classical HR-SAFT EOS with the same set of parameters as in the HRX-SAFT, but with the zero value of the Ginzburg number. As one can see, far away from the critical point at low pressures both equations (HRX/ASN- and HRX-SAFT) practically coincide. Comparison of the predictions of the HRX/ASN-SAFT model with experimental data at other isotherms is shown in Figures 2 and 3. For calculation of the VLE properties of the mixtures, we used an iterative algorithm developed by Lemmon.[70] As pointed out in ref 47, this algorithm does not converge very close to the critical point of a mixture, for example, when $|T/Tc - 1| \leq 10^{-2}$, and

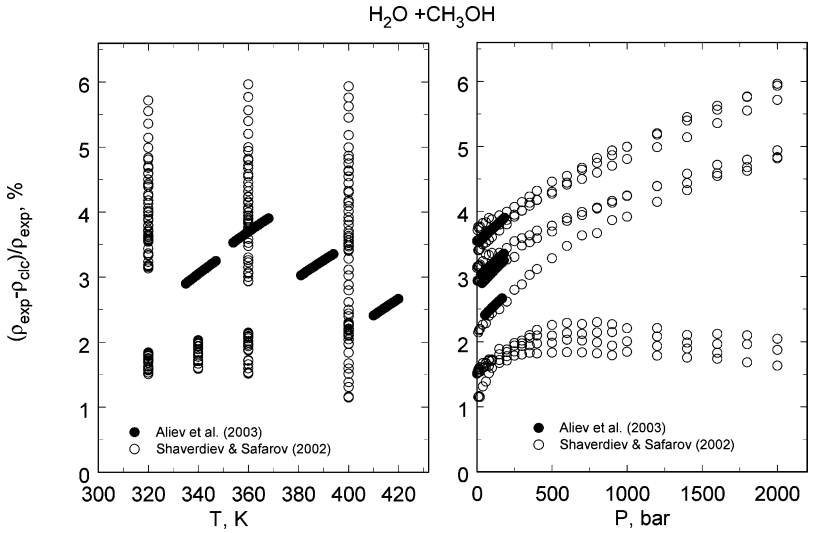

Figure 5. Deviations between experimental densities obtained for the water + methanol mixture by Shahverdiev and Safarov[71] (empty symbols) and by Aliev et al.[72] (filled symbols) and the values calculated with the HRX/ASN-SAFT EOS.

alternative algorithms should be used. Thus, the calculations of the HRX models shown Figure 2 do not go all the way to the critical point. As we mentioned above, the more-rigorous way of representing the thermodynamic surface of binary mixtures in the critical region is a formulation of the crossover equation of state for mixtures in terms of the field variable μ rather than x. In this case, the parameters T_c, P_c, and v_c in eqs 18 and 19 are the real critical parameters of a mixture, determined from the critical-point conditions

$$\left(\frac{\partial \mu}{\partial x}\right)_{T_c,P_c} = 0, \quad \left(\frac{\partial^2 \mu}{\partial x^2}\right)_{T_c,P_c} = 0, \quad \left(\frac{\partial^3 \mu}{\partial x^3}\right)_{T_c,P_c} > 0 \qquad (28)$$

and we would expect better convergence of our algorithm in the near-critical region. However, as one can see, even in the present formulation, contrary to the HR-SAFT EOS, both the HRX/ASN- and HRX-SAFT models not only give a much better description of the $P - x$ data in the critical region but also reproduce the $P - \rho$ data with high accuracy.

The second system considered here is the water + methanol mixture. In our previous work,[53] all system-dependent parameters for this mixture were found from a fit of the HRX -SAFT EOS to one-phase *PVTx* data obtained by Shahverdiev and Safarov[71] and by Aliev et al.[72] and were then used for calculating of other properties for this mixture. In this work, all system-dependent coefficients for this mixture have been found from a fit of the HRX/ASN-SAFT EOS to the excess molar enthalpy, H_m^E, data obtained by Wormald et al.[73] Comparisons of the HRX/ASN-SAFT predictions with experimental excess molar enthalpy, H_m^E, data for the water + methanol mixtures are shown in Figure 4. Again, both the HRX/ASN and HRX-SAFT models give very similar results. At low temperatures and moderate pressures, good agreement of the predicted and experimental values is observed. At higher temperatures, the deviations between calculated and experimental values of the excess molar enthalpy are larger.

The comparisons of the HRX/ASN-SAFT predictions and experimental densities for the water + methanol mixture are shown in Figure 5. The empty symbols in Figure 5 indicate the data of Shahverdiev and Safarov[71] and the filled symbols correspond to the data obtained by Aliev et al.[72] In wide range of pressures, up to 2000 bar, the maximum deviations do not exceed 6%. We note that these results are slightly worse that results obtained with the HRX-SAFT (about 3%). However, because these data have not been used for the optimization of the HRX/ASN EOS (and were used to optimize the HRX-SAFT model), we consider the agreement between experimental data and calculated values of the densities to be good.

4. Conclusions

In this work, we incorporated a new analytical formulation for the crossover function[58] into the crossover HRX-SAFT EOS for fluid mixtures.[53] Thus, we have developed an analytical crossover HRX/ASN-SAFT equation of state for mixtures of associating fluids. We show that the new HRX/ASN-SAFT equation of state reproduces experimental data in binary mixtures with approximately the same accuracy as the original HRX-SAFT equation of state but is much more simple and convenient for practical calculations. The systems studied were restricted to binary mixtures with continuous critical curves (type-I phase behavior). Application of the HRX/ASN-SAFT EOS to mixtures with more-complicated, higher types of phase behavior is underway and will be reported in future publications.

Appendix

The third-order derivatives of the fractions of nonbonded associating molecules

$$[\Lambda_{\mathbf{pq}}]\left(\frac{\partial^3}{\partial\xi\partial\omega\partial\theta}[X_i^j]\right) = [\Psi_{\mathbf{p}}^{\xi\omega\theta}]$$

1. With respect to density: $\partial^3 X_i^j/\partial\rho^3$

$$\Psi_{\mathbf{p}}^{\rho\rho\rho} = \frac{3}{\rho}\frac{\partial^2 X^j_i}{\partial\rho^2} - \frac{6}{\rho^3}X^j_i(1 - X^j_i) + \frac{6}{X^j_i}\left(\frac{\partial X^j_i}{\partial\rho}\frac{\partial^2 X^j_i}{\partial\rho^2} - \frac{1}{X^j_i}\left(\frac{\partial X^j_i}{\partial\rho}\right)^3\right) - \frac{6}{\rho}\frac{\partial X^j_i}{\partial\rho}\left(\frac{1}{\rho} + \frac{1}{X^j_i}\frac{\partial X^j_i}{\partial\rho}\right) - \rho(X^j_i)^2\sum_{k=1}^{n}x_k\sum_{l=1,l\neq j}^{s}S^l_k\left(X^l_k\frac{\partial^3\Delta^{lj}_{ki}}{\partial\rho^3} + 3\frac{\partial^2\Delta^{lj}_{ki}}{\partial\rho^2}\frac{\partial X^l_k}{\partial\rho} + 3\frac{\partial\Delta^{lj}_{ki}}{\partial\rho}\frac{\partial^2 X^l_k}{\partial\rho^2}\right)$$

2. With respect to density and temperature: $\partial^3 X_i^j/\partial\rho\partial T^2$

$$\Psi_{\mathbf{p}}^{\rho TT} = \frac{1}{\rho}\frac{\partial^2 X_i^j}{\partial T^2} - \frac{2}{\rho X_i^j}\left(\frac{\partial X_i^j}{\partial T}\right)^2 + \frac{2}{X_i^j}\left(\frac{\partial X_i^j}{\partial \rho}\frac{\partial^2 X_i^j}{\partial T^2} - \frac{3}{X_i^j}\frac{\partial X_i^j}{\partial \rho}\left(\frac{\partial X_i^j}{\partial T}\right)^2 + 2\frac{\partial X_i^j}{\partial T}\frac{\partial^2 X_i^j}{\partial \rho \partial T}\right) - \rho(X_i^j)^2 \sum_{k=1}^{n} x_k \sum_{l=1,l\neq j}^{s} S_k^l \left(X_k^l \frac{\partial^3 \Delta_{ki}^{lj}}{\partial\rho\partial T^2} + 2\frac{\partial^2 \Delta_{ki}^{lj}}{\partial\rho\partial T}\frac{\partial X_k^l}{\partial T} + 2\frac{\partial \Delta_{ki}^{lj}}{\partial T}\frac{\partial^2 X_k^l}{\partial\rho\partial T} + \frac{\partial X_k^l}{\partial\rho}\frac{\partial^2 \Delta_{ki}^{lj}}{\partial T^2} + \frac{\partial \Delta_{ki}^{lj}}{\partial\rho}\frac{\partial^2 X_k^l}{\partial T^2}\right)$$

References and Notes

(1) Jackson, G.; Chapman, W. G.; Gubbins, K. E. *Mol. Phys.* **1988**, *65*, 1.
(2) Chapman, W. G.; Gubbins, K. E.; Jackson, G.; Radosz, M. *Fluid Phase Equilib.* **1989**, *52*, 31.
(3) Chapman, W. G.; Gubbins, K. E.; Jackson, G.; Radosz, M. *Ind. Eng. Chem. Res.* **1990**, *29*, 1709.
(4) Fu, Y.-H.; Sandler, S. I. *Ind. Eng. Chem. Res.* **1995**, *34*, 1897.
(5) Huang, S. H.; Radosz, M. *Ind. Eng. Chem. Res.* **1990**, *29*, 2284.
(6) Huang, S. H.; Radosz, M. *Ind. Eng. Chem. Res.* **1991**, *30*, 1994.
(7) Huang, S. H.; Radosz, M. *Fluid Phase Equilib.* **1991**, *70*, 33.
(8) Kraska, T.; Gubbins, K. E. *Ind. Eng. Chem. Res.* **1996**, *35*, 4738.
(9) Kraska, T.; Gubbins, K. E. *Ind. Eng. Chem. Res.* **1996**, *35*, 4727.
(10) Wertheim, M. S. *J. Stat. Phys.* **1984**, *35*, 19.
(11) Wertheim, M. S. *J. Stat. Phys.* **1984**, *35*, 35.
(12) Wertheim, M. S. *J. Stat. Phys.* **1986**, *42*, 459.
(13) Wertheim, M. S. *J. Stat. Phys.* **1986**, *42*, 477.
(14) Muller, E. A.; Gubbins, K. E. *Ind. Eng. Chem. Res.* **2001**, *40*, 2193.
(15) Paricaud, P.; Galindo, A.; Jackson, G. *Fluid Phase Equilib.* **2002**, *194*−197, 87.
(16) Albright, P. C.; Sengers, J. V.; Nicoll, J. F.; Ley-Koo, M. *Int. J. Thermophys.* **1986**, *7*, 75.
(17) Depablo, J. J.; Prausnitz, J. M. *Fluid Phase Equilib.* **1990**, *59*, 1.
(18) Erickson, D. D.; Leland, T. W. *Int. J. Thermophys.* **1986**, *7*, 911.
(19) Fornasiero, F.; Lue, L.; Bertucco, A. *AIChE J.* **1999**, *45*, 906.
(20) Fox, J. R. *Fluid Phase Equilib.* **1983**, *14*, 45.
(21) Fox, J. R.; Storvick, T. S. *Int. J. Thermophys.* **1990**, *11*, 49.
(22) Jiang, J.; Prausnitz, J. M. *J. Chem. Phys.* **1999**, *111*, 5964.
(23) Jiang, J.; Prausnitz, J. M. *Fluid Phase Equilib.* **2000**, *169*, 127.
(24) Kostrowichka Wysolkovska, A.; Anisimov, M. A.; Sengers, J. V. *Fluid Phase Equilibr*. **1999**, *158*−160, 523.
(25) Kraska, T.; Deiters, U. K. *Int. J. Thermophys.* **1994**, *15*, 261.
(26) Leonhard, K.; Kraska, T. *J. Supercrit. Fluids* **1999**, *16*, 1.
(27) Lue, L.; Praustitz, J. M. *J. Chem. Phys.* **1998**, *108*, 5529.
(28) Lue, L.; Praustitz, J. M. *AIChE J.* **1998**, *44*, 1455.
(29) Parola, A.; Meroni, A.; Reatto, L. *Int. J. Thermophys.* **1989**, *10*, 345.
(30) Parola, A.; Reatto, L. *Phys. Rev. Lett.* **1984**, *53*, 2417.
(31) Parola, A.; Reatto, L. *Phys. Rev. A* **1985**, *31*, 3309.
(32) Pini, D.; Parola, A.; Reatto, L. *Int. J. Thermophys.* **1998**, *19*, 1545.
(33) Pini, D.; Stell, G.; Wilding, N. B. *Mol. Phys.* **1998**, *95*, 483.
(34) Reatto, L.; Parola, A. *J. Phys.: Condens. Matter* **1996**, *8*, 9221.
(35) Tang, Y. P. *J. Chem. Phys.* **1998**, *109*, 5935.
(36) Tau, M.; Parola, A.; Pini, D.; Reatto, L. *Phys. Rev. E* **1995**, *52*, 2644.
(37) van Pelt, A.; Jin, G. X.; Sengers, J. V. *Int. J. Thermophys.* **1994**, *15*, 687.
(38) White, J. A. *J. Chem. Phys.* **1999**, *111*, 9352.
(39) White, J. A. *J. Chem. Phys.* **2000**, *112*, 3236.
(40) White, J. A. *Int. J. Thermophys.* **2001**, *22*, 1147.
(41) White, J. A.; Zhang, S. *J. Chem. Phys.* **1990**, *103*, 1922.
(42) White, J. A.; Zhang, S. *J. Chem. Phys.* **1993**, *99*, 2012.
(43) Kiselev, S. B.; Ely, J. F. *Ind. Eng. Chem. Res.* **1999**, *38*, 4993.
(44) Kiselev, S. B. *Fluid Phase Equilib.* **1998**, *147*, 7.
(45) Kiselev, S. B.; Ely, J. F. *J. Chem. Phys.* **2003**, *119*, 8645.
(46) Kiselev, S. B.; Ely, J. F. *Fluid Phase Equilib.* **2004**, *222*−223, 149.
(47) Kiselev, S. B.; Friend, D. G. *Fluid Phase Equilib.* **1999**, *162*, 51.
(48) Kudelkova, L.; Lovland, J.; Vonka, P. *Fluid Phase Equilib.* **2004**, *218*, 103.
(49) Hu, Z. Q.; Yang, J. C.; Li, Y. G. *Fluid Phase Equilib.* **2003**, *205*, 1.
(50) Hu, Z. Q.; Yang, J. C.; Li, Y. G. *Fluid Phase Equilib.* **2003**, *205*, 25.
(51) Kiselev, S. B.; Ely, J. F.; Abdulagatov, I. M.; Magee, J. W. *Int. J. Thermophys.* **2000**, *6*, 1373.
(52) Kiselev, S. B.; Ely, J. F.; Adidharma, H.; Radosz, M. *Fluid Phase Equilib.* **2001**, *183*, 53.
(53) Kiselev, S. B.; Ely, J. F.; Tan, S. P.; Adidharma, H.; Radosz, M. *Ind. Eng. Chem. Res.* **2006**, *45*, 3981.
(54) McCabe, C.; Kiselev, S. B. *Ind. Eng. Chem. Res.* **2004**, *43*, 2839.
(55) McCabe, C.; Kiselev, S. B. *Fluid Phase Equilib.* **2004**, *219*, 3.
(56) Sun, L.; Kiselev, S. B.; Ely, J. F. *Fluid Phase Equilib.* **2005**, *233*, 204.
(57) Kiselev, S. B.; Ely, J. F. *Fluid Phase Equilib.* **2000**, *174*, 93.
(58) Kiselev, S. B.; Ely, J. F. *Chem. Eng. Sci.* **2006**, *61*, 5107.
(59) Mansoori, G. A.; Carnahan, N. F.; Starling, K. E.; Leland, T. W., Jr. *J. Chem. Phys.* **1971**, *54*, 1523.
(60) Chen, S. S.; Kreglewski, A. *Ber. Bunsen-Ges. Phys. Chem.* **1977**, *81*, 1048.
(61) Tan, S. P.; Adidharma, H.; Radosz, M. *Ind. Eng. Chem. Fundam.* **2004**, *43*, 203.
(62) Anisimov, M. A.; Kiselev, S. B. Universal Crossover Approach to Description of Thermodynamic Properties of Fluids and Fluid Mixtures. In *Sov. Tech. Rev. B. Therm. Phys., Part 2*; Scheindlin, A. E., Fortov, V. E., Eds.; Harwood Academic: New York, 1992; Vol. 3; p 1.
(63) Sengers, J. V.; Levelt Sengers, J. M. H. *Annu. Rev. Phys. Chem.* **1986**, *37*, 189.
(64) Kiselev, S. B.; Ely, J. F.; Adidharma, H.; Radosz, M. *Fluid. Phase. Equilib.* **2000**, *183*−*184*, 53.
(65) Fisher, M. *Phys. Rev. B* **1968**, *176*, 257.
(66) Griffiths, R. B.; Wheeler, J. C. *Phys. Rev. A* **1970**, *2*, 1047.
(67) Saam, W. F. *Phys. Rev. A* **1970**, *2*, 1461.
(68) Button, J. K.; Gubbins, K. E. *Fluid Phase Equilib.* **1999**, *158*−160, 175.
(69) Brunner, E.; Hueltenschmidt, W.; Schlichthaerle, G. *J. Chem. Thermodyn.* **1987**, *19*, 273.
(70) Lemmon, E. A Generalized Model for the Prediction of the Thermodynamic Properties of Mixtures including Vapor-Liquid Equilibrium. Ph.D. Thesis, University of Idaho, 1996.
(71) Shahverdiev, A. N.; Safarov, J. T. *Phys. Chem. Chem. Phys.* **2002**, *4*, 979.
(72) Aliev, M. M.; Magee, J. W.; Abdulagatov, I. M. *Int. J. Thermophys.* **2003**, *24*, 1527.
(73) Wormald, C. J.; Badock, L.; Lloyd, M. J. *J. Chem. Thermodyn.* **1996**, *23*, 603.
(74) Leu, A.-D.; Chung, S. Y.-K.; Robinson, D. B. *J. Chem. Thermodyn.* **1991**, *23*, 979.